Dynamics of reaction-diffusion systems in a subdiffusive regime

D. Hernández, C. Varea, and R. A. Barrio
Instituto de Fisica, Universidad Nacional Autónoma de México (UNAM), Apartado Postal 20-364 01000 México, D.F., Mexico
(Received 18 September 2008; revised manuscript received 10 November 2008; published 20 February 2009)

In this paper, we examine the dynamics of reaction-diffusion systems with fractional time derivatives. It is shown that in these conditions diffusion is anomalous, in the sense that the mean-square displacement $\langle r^2 \rangle \sim t^{\gamma}$, where $\gamma < 1$, a situation known as subdiffusion. We study the conditions for the appearance of a diffusion-driven instability and show that the restrictive conditions for a Turing instability are relaxed. This implies that systems whose kinetics are not of the activator-inhibitor kind can have a Turing instability and a modulated final state. We demonstrate our results with numerical calculations in two dimensions using a generic Turing model.

DOI: 10.1103/PhysRevE.79.026109 PACS number(s): 82.20.−w, 82.56.Lz, 05.20.−y

I. INTRODUCTION

In 1952, Alan Turing [1] first pointed out that stable stationary spatial patterns could be a result of a diffusion-driven instability, and that many facts in morphogenesis could be understood by this mechanism. The equations that Turing proposed are coupled nonlinear partial differential equations known as reaction-diffusion systems, in which chemical substances, or morphogens, diffuse in a medium and react chemically among themselves. There are many reaction-diffusion models that have been expressly made to study specific phenomena in chemistry [2], ecology [3], and biology [4], and in many of them there exists the possibility of a Turing instability (for a review, see [5]).

Among the conditions that must be met in order to promote a Turing instability in a two-component activator-inhibitor system are that the trace of the Jacobian must be negative and that the diffusion constants should be very different. The latter condition is very difficult to meet in real systems, and it was not until 1990 that a chemical reactor producing spatial patterns through a Turing instability was realized in the laboratory (CIMA reaction) [6].

Finding chemicals that diffuse differently in a medium, together with the difficulty of identifying morphogens in complicated systems, prevented the detection of Turing patterns in real biological systems for a long time. One of the first indications that the Turing mechanism could explain the pattern on the skin of some marine fish was published in 1995 [7], but it was not until 2006 that it was demonstrated experimentally that the pattern of folicles on the skin of mice most certainly is produced by a Turing instability [8].

The formation of Turing patterns in systems with anomalous diffusion has been studied before. The regime of superdiffusion has been modeled with spatial fractional derivatives in the asymmetrical case, and in curved surfaces [9]. The interesting results are that Turing patterns acquire a velocity that depends on the anomalous diffusion exponent, and that the range of diffusion coefficients ratio (D) in which Turing patterns appear is wider, to the extreme that even when $D=1$, Turing patterns are predicted. This obviously increases the potential applicability of Turing models to real situations.

Subdiffusion has acquired relevance in the past decades because it has been detected experimentally in several systems, such as porous media [10], glasses [11], transport through cell membranes [12,13], and other biological systems [14]. Contrary to the case of superdiffusion [15,16], modeling chemical reactions in the presence of time fractional derivatives is still an open question [17,18]. The problem of modeling subdiffusion with time fractional derivatives is that, under a similar hypothesis about chemical reactions, it is possible to derive various reaction subdiffusion equations whose properties and solutions are totally different [18].

Studies of subdiffusion in reaction-diffusion systems using time fractional derivatives [19] have shown that the conditions for a Turing instability are not different from the usual conditions for special cases of subdiffusion [20]. Here we show that there is a new way of obtaining Turing patterns with subdiffusion. Furthermore, we analyze the general situation of two-component systems with different anomalous exponents.

This paper is organized as follows. In Sec. II, we make a brief description of the state of the art in modeling anomalous diffusion with fractional derivatives, and mention some of the real systems that might be suitable to be treated with these tools. In Sec. III, we describe in detail the modeling of subdiffusion with fractional time derivatives. In Sec. IV, we analize a two-component reaction-diffusion system and give general conditions for a Turing instability to appear. In Sec. V, we demonstrate the predictions of the analysis by exhibiting numerical calculations in a generic Turing model used by us before [21], and in Sec. VI we summarize our results and draw some conclusions.

II. ANOMALOUS DIFFUSION AND FRACTIONAL DERIVATIVES

Diffusion is a common phenomenon in Nature and is a mechanism of transport that reflects the physical properties of the system in which it takes place, as the temperature, the space dimensions, the geometrical structure of the domain in which it happens, and the type of interactions between the diffusive substance and the medium. The connection between diffusion and the microscopic components of matter was first explained by Einstein [22], and an essential ingredient of his explanation is that the process is basically sto-

TABLE I. Different types of diffusion.

		Selected examples	Mathematical treatment[a]	Equation
Normal $\langle x^2\rangle \sim t$	Diffusion	Most physical, chemical, and biological systems	Random walk $\rightarrow$ CLT$\rightarrow$Fick's law	$\partial_t \phi = D\nabla^2\phi$
Anomalous $\langle x^2\rangle \sim t^\alpha$	Subdiffusion $\alpha<1$	Disordered solids Porous media	CTRW $\rightarrow$ Power-law waiting time	$\partial_t^\alpha \phi = D\nabla^2\phi$ $0<\alpha<1$
		Biological tissues Transport through cell membranes	distributions $\rightarrow$ Fick's law with memory effects	(time fractional derivatives)
Anomalous $\langle x^2\rangle \sim t^\alpha$	Superdiffusion $\alpha>1$	Plasma physics Chaotic dynamics Turbulence Transport in polymers	CTRW+Lèvy flights $\rightarrow$ generalized CLT $\rightarrow$ nonlocal Fick's law.	$\partial_t \phi = D\nabla_s^\alpha\phi$ $1<\alpha<2$ (space fractional derivatives)
		Epidemics and foraging	Correlated random walks and Lèvy walks	Probabilistic master equations

[a]CLT denotes Central limit theorem; CTRW denotes continuous-time random walk.

chastic, due to the enormous number of particles involved in the transport process. Because of the central limit theorem, the random walks performed by these particles produce a normal distribution for their positions at times long compared with the mean time interval between successive jumps, which implies that the mean-square displacement grows as $\langle r^2\rangle \propto t$. Most diffusion processes obey this law. However, around 1926, Richardson [23] found that diffusion in turbulent media is anomalous, since $\langle r^2\rangle$ does not grow linearly with time, and by the 1960s many other systems were found to exhibit anomalous diffusion. A good example is the diffusion of charged particles in amorphous solids [24].

In 1965, Montroll and Weiss [25] introduced the concept of continuous-time random walks (CTRW) as a possible explanation of anomalous diffusion [26,27]. In the 1990s it was realized that, under certain circumstances, the CTRW formalism is equivalent to a macroscopic description of the walkers density by a generalized diffusion equation, in which the differential operators are replaced by fractional derivatives [28–30].

In general, anomalous diffusion is characterized by [26]

$$\langle r(t)^2\rangle \propto t^\gamma, \quad \gamma \neq 1,$$

$$\langle r(t)^2\rangle \propto t\ln(t), \tag{1}$$

where the anomalous exponent is $\gamma>1$ for superdiffusion and $\gamma<1$ for subdiffusion. These expressions obviously imply that the central limit theorem is not fulfilled, but generalized concepts, such as Lèvy distributions [26,31], allow us to derive evolution equations for these kinds of phenomena.

In Table I, we summarize the situation related to anomalous diffusion and give some examples of real systems in which each type of anomalous diffusion appears.

III. SUBDIFFUSION MODELED WITH TIME FRACTIONAL DERIVATIVES

Let us start by briefly reviewing the basic relation between continuous-time random walks and anomalous diffusion. Suppose that in a random walk the time between two steps is a random variable τ defined by a probability distribution $\psi(\tau)$. Then the time to take N steps is $t=\Sigma_{i=1}^N \tau_i$, and the probability to find the walker in position X at time t (if it was at $X=0$ when $t=0$) is

$$P(X,t) = \delta(X)\int_t^\infty \psi(\tau)d\tau + \int_0^t\int_{-\infty}^\infty \zeta(X-x,t-\tau)P(x,\tau)dxd\tau, \tag{2}$$

where $\zeta(X-x,t-\tau)$ is the probability that a step of size $X-x$ takes place after a waiting time of $t-\tau$ in the time interval $(\tau,\tau+d\tau)$. In this case, the step and waiting time distributions are given by

$$\lambda(x) = \int_0^\infty \zeta(x,t)dt,$$

$$\psi(t) = \int_{-\infty}^\infty \zeta(x,t)dx. \tag{3}$$

Taking the Fourier and Laplace transforms of Eq. (2), we obtain

$$\hat{\tilde{P}}(k,s) = \frac{1-\hat{\psi}(s)}{s}\frac{1}{1-\hat{\tilde{\zeta}}(k,s)}, \tag{4}$$

and assuming that the steps and the time intervals are independent variables, we may write $\zeta(x,t)=\lambda(x)\psi(t) \Rightarrow \hat{\tilde{\zeta}}(k,s) = \tilde{\lambda}(k)\hat{\psi}(s)$, which could be substituted into Eq. (4) to obtain

$$\tilde{\hat{P}}(k,s) = \frac{1-\hat{\psi}(s)}{s}\frac{1}{1-\tilde{\lambda}(k)\hat{\psi}(s)}. \tag{5}$$

If the first moment of $\psi(t)$ and the second moment of $\lambda(x)$ do not exist, and furthermore

$$\psi(t) \sim t^{-(1+\beta)}, \quad t \gg 1, \quad 0<\beta<1, \tag{6}$$

$$\lambda(x) \sim |x|^{-(1+\gamma)}, \quad x \gg 1, \quad 1<\gamma<2, \tag{7}$$

then it can be shown from Eq. (5) that the time evolution of the probability density reduces to

$$\frac{{}^{c}\partial^{\beta}P(X,t)}{\partial t^{\beta}} = D_{\gamma,\beta}\frac{\partial^{\gamma}P(X,t)}{\partial|X|^{\gamma}},$$

$$P(X,0) = \delta(X),$$

$$0<\beta\leqslant 1, \quad 1<\gamma\leqslant 2, \tag{8}$$

which is a generalized symmetric diffusion equation. In here the time operator is the Caputo fractional derivative of order β [32], and the spatial operator is the Riemann-Liouville fractional derivative of order γ [28,29,33]. The explicit form of these operators in one-dimensional systems is

$$\frac{{}^{c}\partial^{\beta}P(X,t)}{\partial t^{\beta}} = \frac{1}{\Gamma(1-\beta)}\int_0^t (t-\tau)^{-\beta}\frac{\partial P(X,\tau)}{\partial\tau}d\tau,$$

$$\frac{\partial^{\gamma}P(X,t)}{\partial|X|^{\gamma}} = \frac{1}{\Gamma(2-\gamma)}\frac{\partial^2}{\partial X^2}\int_{-\infty}^{\infty}|X-Y|^{1-\gamma}P(Y,t)dY,$$

$$0<\beta\leqslant 1, \quad 1<\gamma\leqslant 2. \tag{9}$$

Subdiffusion can be modeled as a special case of Eq. (8),

$$\frac{{}^{c}\partial^{\beta}P(X,t)}{\partial t^{\beta}} = D_{\beta}\nabla^2 P(X,t),$$

$$0<\beta\leqslant 1, \tag{10}$$

if the waiting time distribution is given by Eq. (6), and the second moment of the jump probability distribution is finite. This type of situation could arise when there are regions in the diffusive medium where the walker could be trapped [26,34]. Another way of obtaining Eq. (10) is by the use of fractional master equations [35], in which the time derivative of the probability distribution is substituted by a fractional derivative of order $\beta \in (0,1)$. It is worth pointing out that some authors [28,29,32,36] say that Eq. (6) is a sufficient condition to obtain Eq. (10). However, there are studies [37] that show that it is only necessary. Fourier transforming Eq. (10), we obtain

$$\frac{{}^{c}\partial^{\beta}\tilde{P}(k,t)}{\partial t^{\beta}} = -D_{\beta}k^2\tilde{P}(k,t), \tag{11}$$

whose solution is $\tilde{P}(k,t)=E_{\beta}(-D_{\beta}k^2t^{\beta})$. The Mittag-Leffler function of order β [38,39] can be written as a series,

$$E_{\beta}(z) = \sum_{n=0}^{\infty}\frac{z^n}{\Gamma(\beta n+1)}, \tag{12}$$

which could be interpreted as a generalization of the exponential function. Now, multiplying Eq. (10) by x^2 and integrating over all the domain, we get

$$\frac{{}^{c}\partial^{\beta}\langle x^2\rangle}{\partial t^{\beta}} = 2D_{\beta}, \tag{13}$$

which implies that

$$\langle x^2\rangle = \frac{2D_{\beta}}{\Gamma(1+\beta)}t^{\beta},$$

$$0<\beta\leqslant 1, \tag{14}$$

recovering the characteristic behavior of subdiffusion.

IV. ANALYSIS OF A GENERAL REACTION-DIFFUSION SYSTEM WITH TWO COMPONENTS

In this section, we shall investigate the effects of subdiffusion in reaction-diffusion systems with two morphogens. As mentioned before, one way of doing this is to write the reaction-diffusion equations with fractional derivatives in time [9,17,40]. There have been studies analyzing the modeling of the reactive part in the presence of subdiffusion [18,20,41], but there are still many interesting things to be discovered.

A dimensionless two-chemical reaction-diffusion system can be written as

$$\frac{\partial u}{\partial t} = D\nabla^2 u + \eta f(u,v),$$

$$\frac{\partial v}{\partial t} = \nabla^2 v + \eta g(u,v), \tag{15}$$

where u and v are related to the concentrations of two chemicals, while f and g are nonlinear functions representing the kinetics of the chemical reactions. Observe that the distance and time are also dimensionless quantities, measured in units given by η. Usual linear stability analysis at $k=0$ takes out all effects of diffusion, which is not necessarily the case when anomalous diffusion is present. In the case of subdiffusion-controlled chemical reactions, it has been shown [18,42–44] that the standard reaction kinetics, as derived from the law of mass action, is not applicable. A suitable model for this situation can be written as

$$\frac{{}^{c}\partial^{\alpha}u}{\partial t^{\alpha}} = D\nabla^2 u + \eta f(u,v),$$

$$\frac{{}^{c}\partial^{\beta}v}{\partial t^{\beta}} = \nabla^2 v + \eta g(u,v),$$

$$0<\alpha, \quad \beta\leqslant 1. \tag{16}$$

Note that in this form the evolution of the uniform state is controlled by subdiffusion, even if the spatial term is not present ($k=0$). Considering the CTRW, there is a problem to describe chemical reactions in the presence of subdiffusion, because the kinetics could take place during the waiting times, or not. This is reflected in the presence of time fractional derivatives acting on the reacting terms [17,20]. The model in Eq. (16) corresponds to the one thoroughly studied by Langlands *et al.* [20], who showed that when $\alpha=\beta<1$, a Turing instability exists, and that the conditions for its appearance are the same as for the normal reaction-diffusion systems. They also showed that the patterns produced are very similar in both cases. Although we agree with these results, we shall show that the Turing conditions could be met in new situations, previously undetected.

Also for $\alpha=\beta<1$, Gafiychuk *et al.* [19,40,45] pointed out that the anomalous exponent is a bifurcation parameter with a certain critical value α_c that separates a regime of stationary Turing patterns from an oscillatory cellular instability, more commonly known as a Hopf-Turing bifurcation.

Using a generalization of Eq. (16), Nec and Nepomnyashchy [46] studied an activator-inhibitor model where fractional derivatives of different exponents act both on diffusion and reaction terms. They show that for a Turing instability to exist, the system must fulfill more severe restrictions than the analogue for normal reaction-anomalous diffusion.

Finally, it is important to mention Yadav and Horsthemke's work [47]. Their model for chemical reactions, in the activation-controlled limit in the presence of subdiffusion, has the property that the Turing instability persists, but the characteristic band of unstable modes and critical diffusion coefficient ratio are both modified due to memory effects in the transport process. It is interesting to mention that in this model, unlike Eq. (16), reaction and subdiffusion processes are not separable, which means that the non-Markovian nature of subdiffusion results in a nontrivial combination of reactions and spatial dispersal.

Although the linear analysis of the model of Eq. (16) has been published elsewhere [17,19,40,45], it is convenient to write it down here in detail in order to appreciate the new results that emerge from it.

Linearizing around a fixed point and setting the scale factor $\eta=1$ for simplicity, we may write

$$\frac{{}^{c}\partial^{\alpha}u}{\partial t^{\alpha}} = D\nabla^2 u + a_{11}u + a_{12}v,$$

$$\frac{{}^{c}\partial^{\beta}v}{\partial t^{\beta}} = \nabla^2 v + a_{21}u + a_{22}v, \tag{17}$$

where a_{ij} are the elements of the Jacobian of the kinetics. Applying Fourier and Laplace transforms to Eq. (17), we obtain

$$s^{\alpha}U - s^{\alpha-1}U(k,0) = -Dk^2U + a_{11}U + a_{12}V,$$

$$s^{\beta}V - s^{\beta-1}V(k,0) = -k^2V + a_{21}U + a_{22}V, \tag{18}$$

where U and V are given by

$$U = \int_{-\infty}^{\infty}\int_0^{\infty} e^{ikx}e^{-st}u(x,t)dtdx = \mathcal{F}(\mathcal{L}(u)),$$

$$V = \int_{-\infty}^{\infty}\int_0^{\infty} e^{ikx}e^{-st}v(x,t)dtdx = \mathcal{F}(\mathcal{L}(v)).$$

Solving the system of Eqs. (18), we get

$$U(k,s) = \frac{(s^{\beta}+Dk^2-a_{22})s^{\alpha-1}U(k,0) + s^{\beta-1}a_{12}V(k,0)}{S(k,s)},$$

$$V(k,s) = \frac{(s^{\alpha}+Dk^2-a_{11})s^{\beta-1}V(k,0) + s^{\alpha-1}a_{21}U(k,0)}{S(k,s)}. \tag{19}$$

The time evolution of $u(k,t)=\mathcal{L}^{-1}(U(k,s))$ is given by the singularities of Eq. (19), that is, the zeros of the function

$$S(k,s) = s^{\alpha+\beta} + s^{\beta}(Dk^2-a_{11}) + s^{\alpha}(k^2-a_{22}) - k^2(a_{11}+Da_{22}) + Dk^4 + (a_{11}a_{22}-a_{12}a_{21}). \tag{20}$$

This expression should be used for the instability analysis of the system near the fixed points by solving the equation

$$S(k,s_0) = 0. \tag{21}$$

For any arbitrary values of the anomalous exponents α and β, $s_0(k)$ could be studied numerically as a function of the relevant parameters (scale factors, diffusion coefficient ratios) to determine when instabilities should appear in the system of Eq. (17). In particular, the conditions for a Turing instability are

$$\mathrm{Re}[s_0(k=0)] < 0 \tag{22}$$

and

$$\mathrm{Re}[s_0(k)] > 0 \tag{23}$$

for some $k \neq 0$.

Observe that when $\alpha=\beta$, the Mittag-Leffler functions [see Eq. (12)] are the appropriate extensions of the exponential function. Therefore, $U(k,s)$ and $V(k,s)$ can be written in terms of the Laplace transform of these functions [20]. Doing this, Langlands *et al.* [20] used the asymtotic behavior of the Mittag-Leffler functions to investigate the Turing instability, and concluded that the conditions for a Turing instability are analogous to the ones in normal diffusion. However, we have found that there is a further possibility of having a Turing instability in this case, which was previously undetected. In order to appreciate this, we find it pertinent to explain in detail the complete procedure to obtain the solutions of the model when $\alpha=\beta<1$ using the approach suggested by Gafiychuk *et al.* [40]. We start with the Fourier transform of Eq. (16),

$$\frac{{}^{c}\partial^{\alpha}}{\partial t^{\alpha}}\begin{pmatrix}\tilde{u}\\ \tilde{v}\end{pmatrix} = \begin{pmatrix}-D_{\alpha}k^2+a_{11} & a_{12}\\ a_{21} & -k^2+a_{22}\end{pmatrix}\begin{pmatrix}\tilde{u}\\ \tilde{v}\end{pmatrix} = A(k)\begin{pmatrix}\tilde{u}\\ \tilde{v}\end{pmatrix}. \tag{24}$$

Transforming to the representation (e_1,e_2) in which $A(k)$ is diagonal, we obtain

$$\frac{{}^c\partial^\alpha}{\partial t^\alpha}\begin{pmatrix} e_1 \\ e_2 \end{pmatrix} = \begin{pmatrix} \lambda_1 & 0 \\ 0 & \lambda_2 \end{pmatrix}\begin{pmatrix} e_1 \\ e_2 \end{pmatrix}, \tag{25}$$

where $\lambda_i(k)=|\lambda_i|e^{i\theta_i(k)}$ are the complex eigenvalues of $A(k)$. Therefore, any solution of the system can be written as a linear combination of the eigenvectors,

$$e_i(k,t) = e_i(k,0)f(\lambda_i(k)t) \quad (i=1,2), \tag{26}$$

where $f(\lambda_i t)$ is a function that obeys

$$\frac{{}^c\partial^\alpha f(\lambda_i t)}{\partial t^\alpha} = \lambda_i f(\lambda_i t),$$

$$f(0) = 1, \tag{27}$$

whose solutions are the Mittag-Leffler functions $E_\alpha(\lambda t^\alpha)$. Instead of using directly the asymptotic properties of these functions, we shall obtain their explicit form by applying Laplace transform techniques. From the results of the Appendix, we can write the solutions of Eq. (25) as

$$e_i(k,t) = \begin{cases} e_i(k,0)[K(\alpha,\lambda_i(k),t) + I(\alpha,\lambda_i(k),t)] & \text{if } \left|\dfrac{\theta_i(k)}{\alpha}\right| \leq \pi, \\ e_i(k,0)I(\alpha,\lambda_i(k),t) & \text{if } \left|\dfrac{\theta_i(k)}{\alpha}\right| > \pi, \end{cases} \tag{28}$$

where the functions $I(\alpha,\lambda_i(k),t)$ and $K(\alpha,\lambda_i(k),t)$ are the inverse transforms given by Eq. (A10), and are

$$I(\alpha,\lambda_i(k),t) = -\frac{\sin(\pi\alpha)}{\pi}\int_0^\infty \frac{r^{\alpha-1}e^{-|\lambda_i(k)|^{1/\alpha}rt}dr}{e^{-i[\theta_i(k)]}r^{2\alpha} - 2r^\alpha\cos(\pi\alpha) + e^{-i[\theta_i(k)]}},$$

$$K(\alpha,\lambda_i(k),t) = \frac{1}{\alpha}\exp(|\lambda_i(k)|^{1/\alpha}te^{i[\theta_i(k)/\alpha]}), \quad i=1,2. \tag{29}$$

The eigenvalues of the stability matrix $[A(k)]$ are given by

$$\lambda_1 = \frac{\mathrm{Tr}A(k)}{2} + \frac{([\mathrm{Tr}A(k)]^2 - 4h(k))^{1/2}}{2},$$

$$\lambda_2 = \frac{\mathrm{Tr}A(k)}{2} - \frac{([\mathrm{Tr}A(k)]^2 - 4h(k))^{1/2}}{2}, \tag{30}$$

where

$$\mathrm{Tr}A(k) = -k^2(D+1) + (a_{11}+a_{22}),$$

$$h(k) = Dk^4 - k^2(a_{11}+Da_{22}) + \det A(0). \tag{31}$$

From Eq. (29), we can conclude that

$$e_i(k,t) \text{ is } \begin{cases} \text{unstable} & \Leftrightarrow |\theta_i(k)| \leq \dfrac{\pi\alpha}{2}, \\ \text{stable} & \Leftrightarrow |\theta_i(k)| > \dfrac{\pi\alpha}{2}. \end{cases} \tag{32}$$

From here one can see that if both eigenvalues are real and negative ($\theta_i = \pi$), then the system is stable and no Turing instabilities are possible. If both are real and one of them is positive (the other is always negative), then the system becomes unstable, and the conditions for this are exactly the same as for the case $\alpha=1$. However, if the roots are complex ($\theta_i \neq 0,\pi$), then there is a critical value of α for which the solution of Eq. (27) becomes marginally stable [notice that now it is possible for the system to be linearly stable even if $\mathrm{Re}(\lambda_i)>0$], in the sense that for $\alpha<\alpha_c$ the system is stable and if $\alpha>\alpha_c$ it becomes unstable. This critical value α_c only exists if $\mathrm{Tr}A(k)>0$ (since $\theta_i > \frac{\alpha\pi}{2}$ is always fulfilled otherwise) and it is given by

$$\alpha_c(k) = \frac{2}{\pi}\arctan\left(\sqrt{\frac{4h(k)}{[\mathrm{Tr}A(k)]^2} - 1}\right), \tag{33}$$

where the quantities are defined in Eq. (31).

The Turing conditions require the stationary homogeneous state ($k=0$) to be stable, and also that the system should become unstable under perturbations with finite wavelength. According to Eq. (33), when there are chemical reactions in the presence of subdiffusion, the first condition [Eq. (22)] can be satisfied in two ways, either

$$a_{11}+a_{22} < 0,$$

$$a_{11}a_{22} - a_{12}a_{21} > 0, \tag{34}$$

or

$$a_{11}+a_{22} > 0,$$

$$4(a_{11}a_{22} - a_{12}a_{21}) > (a_{11}+a_{22})^2,$$

$$\alpha_c(0) > \alpha, \tag{35}$$

which is impossible for the case of normal diffusion. The difference between these two situations is illustrated in Fig. 1.

When Eq. (34) is fulfilled, α_c does not exist, and to fulfill the condition in Eq. (23) it is necessary that $h(k)<0$, which implies that $(a_{11}+Da_{22})>0$, $D\neq 1$, and $\mathrm{sgn}(a_{11}) \neq \mathrm{sgn}(a_{22})$. This is the result found before [20], and corresponds with the normal conditions for a diffusion-driven instability. It is clear that the critical ratio of diffusion coefficients is exactly the same as for normal diffusion, as its evaluation can be carried out exactly in the same manner. However, when the chemical kinetics satisfy Eq. (35), there are two possibilities for an instability to appear for some $k\neq 0$, depending on the sign of $\mathrm{Tr}A(k)$ and on the value of the anomalous exponent α. On the one hand, it is easy to see from Eqs. (32) that when $\mathrm{Tr}A(k)>0$, the unstable modes must satisfy either

$$4h(k) < [\mathrm{Tr}A(k)]^2 \Rightarrow \mathrm{Im}[\lambda_i(k)] = 0, \quad k \neq 0$$

or

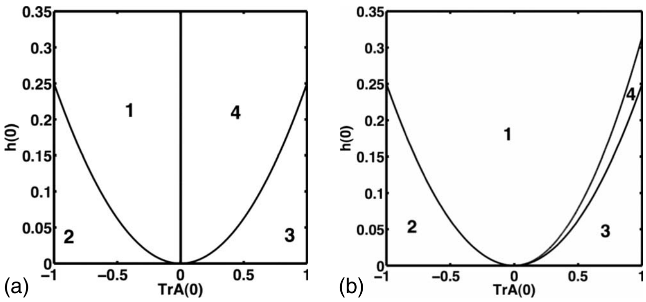

FIG. 1. Stability diagram for the homogeneous state ($k=0$) for (a) normal diffusion and (b) subdiffusion $\alpha_c=0.3919$. The region labeled 1 corresponds to oscillatory stable states, in region 2 there are nonoscillatory stable states, in region 3 there are unstable nonoscillatory states, and in region 4 there are oscillatory unstable states. Notice that the region with possible Turing instabilities is larger for subdiffusion.

$$4h(k) > [\mathrm{Tr}A(k)]^2 \Rightarrow \mathrm{Im}[\lambda_i(k)] \neq 0, \quad \alpha > \alpha_c(k).$$

It is worth noticing that it is possible to have an instability even when $h(k)>0$, which is impossible in the case of normal diffusion. On the other hand, if $\mathrm{Tr}A(k=0)>0$ and $\mathrm{Tr}A(k\neq 0)<0$ for some values of k, then one requires that $h(k\neq)<0$ for an instability to be pumped up. Notice that now the last inequality does not imply that $\mathrm{sgn}(a_{11}) \neq \mathrm{sgn}(a_{22})$. Furthermore, since α_c is a continuous function of k, one could encounter Hopf, Turing, or Turing-Hopf bifurcations. For a pure Turing instability to appear, it is neccesary to fulfill Eq. (22) in all the region where $\mathrm{Tr}[A(k)]\geqslant 0$. Therefore, it is required that

$$\min[\alpha_c(k)] > \alpha \quad \text{for } (0 \leqslant k \leqslant k_0), \tag{36}$$

where k_0 is the wave number in which $\mathrm{Tr}A(k_0)=0$. This minimum is different from zero only if $h(k_0)>0$, in which case $\alpha_c(k)$ is a monotonically increasing function, its minimum value is at $k=0$, and its maximum is $\alpha_c(k_0)=1$.

The physical interpretation of this result is that the stability of the uniform steady states depends not only on the particular characteristics of the reaction, but also on the underlying transport processes. For certain reaction-subdiffusion conditions, an unstable chemical steady state can be stabilized. Regarding the Turing instability as such, this result predicts that stable patterns can be obtained using reaction kinetics that is not necessarily of the activator-inhibitor kind.

In Fig. 2(a), we show a case in which no Turing bifurcation is expected, since the minimum of a_c is zero, while in Fig. 2(b) all the conditions mentioned above are met and a Turing instability is expected.

Finally, we want to stress that the function $S(k,s)$ could be used to investigate numerically the general case of arbitrary anomalous exponents, but only as a guide, since the long-time behavior of the system should be studied with care. In what follows, we shall illustrate the results obtained by dealing with the problem numerically.

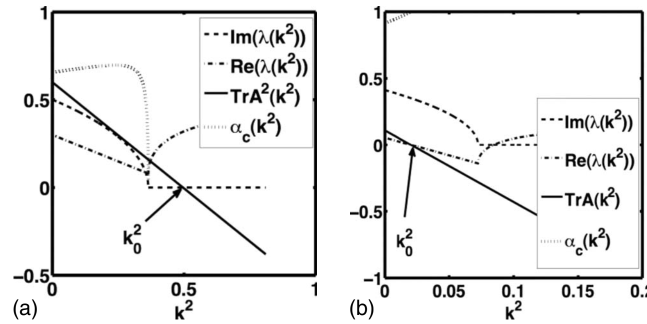

FIG. 2. (a) The imaginary and real parts of λ, $\mathrm{Tr}A$, and α_c as functions of k^2, for $h(k_0)<0$. Notice that $\min(\alpha_c)=0$. (b) The same for $h(k_0)>0$. Notice that α_c is defined only in the region where the trace is positive, and its maximum value is 1.0 at k_0.

V. NUMERICAL CALCULATIONS

Here we study numerically pattern formation with subdiffusion using a reaction-diffusion model put forward by us [21]. This system presents a rich variety of instabilities and has been used in the past to treat various problems in physics and theoretical biology. Its explicit form is

$$\frac{\partial u}{\partial t} = D\delta\nabla^2 u + au(1-r_1v^2) + v(1-r_2u),$$

$$\frac{\partial v}{\partial t} = \delta\nabla^2 v + bv[1+(ar_1/b)uv] + u(\gamma + r_2 v), \tag{37}$$

where the peculiar form of the kinetics is explained elsewhere [21]. To study the appearance of Turing instabilities in the presence of subdiffusion, we shall substitute, the time derivatives by fractional derivatives.

Since the issue of pattern selection is an important one, the numerical calculations were done in two dimensions following the procedure described by Barrio *et al.* [21] concerning the lattice size, the implementation of periodic boundary conditions, and the numerical representation of the spatial derivatives. The system to be integrated in time is

$$\frac{{}^c\partial^\alpha u}{\partial t^\alpha} = D\delta\nabla^2 u + a_{11}u + a_{12}v - r_2uv - (a_{11}r_1)v^2,$$

$$\frac{{}^c\partial^\beta v}{\partial t^\beta} = \delta\nabla^2 v + a_{21}u + a_{22}v + r_2uv + (a_{11}r_1)uv^2,$$

$$0<\alpha, \quad \beta \leqslant 1, \tag{38}$$

where $a_{12}=1$, $\gamma=a_{21}$, $a=a_{11}$, $b=a_{22}$. Observe that this system in general has three fixed points. However, for simplicity we shall set $a_{11}=-a_{21}$, so that there is only one fixed point at $(u,v)=(0,0)$.

We used the discretization of the Caputo fractional derivatives proposed by Gorenflo and Abdel-Rehim [48], namely

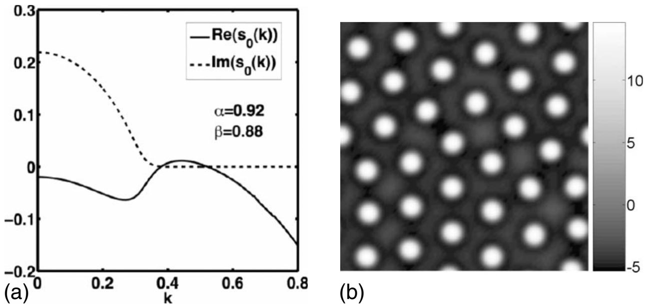

FIG. 3. (a) Zeros of the function $S(k,s)$ for exponents α=0.92, β=0.88. (b) Turing pattern obtained with this set of exponents and nonlinear parameters r_1=0.02 and r_2=0.2, corresponding to spots.

$$\left.\frac{{}^{c}\partial^{\alpha} y_{i,j}}{\partial t^{\alpha}}\right|_{t_{n+1}} = \sum_{m=0}^{n+1} (-1)^k \binom{\alpha}{m} \frac{y_{i,j}(t_{n+1-m}) - y_{i,j}(t_0)}{(\Delta t)^{\alpha}}, \tag{39}$$

where $y_{ij}(t_n)$ is the function evaluated at the point (i,j) in a two-dimensional grid, and at a discrete time t_n. The quantity Δt represents the time step, which was chosen to be 0.01. Observe that the system has a memory of $n+2$ time steps, and there is a need to store all this information in the computer memory. There is a numerical difficulty with the combinatory factors, and much attention should be put in order to avoid losing significant figures with big numbers. This problem was solved by using the recurrence relation

$$\binom{\alpha}{m} = -\left[1 - \frac{1+\alpha}{m}\right]\binom{\alpha}{m-1}. \tag{40}$$

Observe that for m=1, the combinatory factor is α, and the coefficient for m=0 is 1 in Eq. (39). In principle, the number of terms in the summation grows with time, and the calculation becomes rapidly unmanageable. Therefore, in practice we only retain terms whose coefficients are larger than 10^{-7}. In the worse of cases, the number of terms needed in the memory was 800. We found that more terms are needed when the anomalous exponents are smaller.

A. Turing patterns when Tr[$A(k=0)$]<0

We start by observing that, according to linear analysis results, Turing patterns with normal diffusion are formed when a_{11}=0.899, a_{22}=−0.91, a_{12}=1, a_{21}=$-a_{11}$, δ=2, D=0.516. Using these values for the parameters, we are complying with the normal Turing conditions of Eq. (34), and we can calculate explicitly $s_0(k)$ in the case of subdiffusion. For the values α=0.92 and β=0.88, we found that $s_0(k)$ resembles the dispersion relation of a normal Turing system. In Fig. 3(a) we show the plot for $s_0(k)$, and in Fig. 3(b) we show the calculated Turing pattern in a grid of 100×100 with periodic boundary conditions and random initial conditions. The pattern converged after 380 000 time steps with a spatial step dx=1. Notice that, although the anomalous exponents are not equal, Turing patterns appear.

Is important to mention that for different exponents, the homogeneous state (k=0) could be linearly stable or not, depending on how different the exponents are. In Fig. 4, we show an example, keeping the value of α constant. Observe that the real part of $s_0(0)$ is negative when $\alpha-\beta$ is small, and it is positive when large. Former studies [20] concluded that systems with subdiffusion present Turing patterns in the same region where they appear in systems with normal diffusion, when the two anomalous exponents are equal. We find that this region is also achievable when the exponents are different, although the value of the difference has to be small.

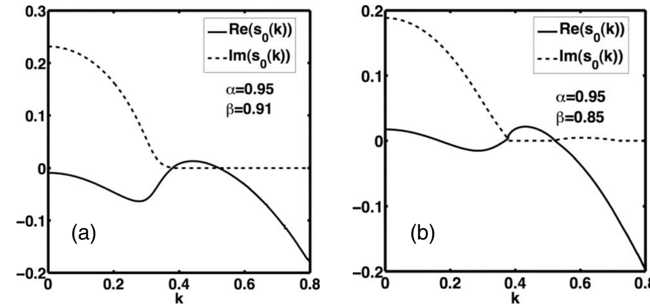

FIG. 4. Zeros of the function $S(k,s)$ for two sets of exponents. (a) $\alpha-\beta$=0.04; (b) $\alpha-\beta$=0.1.

The function $s_0(k)$ is not a dispersion relation in general. However, it provides a good guide to predict the appearance of a Turing instability. For instance, we verified the predictions for k=0 by calculating the phase portrait and we are convinced that the homogeneous state is an attractor for the parameters of Fig. 3 and of Fig. 4(a).

Turing patterns with anomalous diffusion are obtained with the set of linear parameters of Fig. 3, and two different sets of values for the anomalous exponents. This is shown in Fig. 5. Observe that the cubic nonlinearity is predominant and favors stripes while a quadratic one, as in Fig. 3(b), favors spots, as found for normal diffusion [21].

The similarity of the patterns shown in Fig. 5 and Fig. 3(b) with the patterns obtained with normal diffusion is to be expected, since the effect of anomalous diffusion is only felt in the dynamical temporal evolution of the system, and once a Turing pattern is settled the system becomes stationary. Therefore, after convergence, the final patterns should be a solution of the Poisson equation,

$$\nabla^2 u = -\frac{1}{\delta D}[a_{11}u + a_{12}v - r_2 uv - (a_{11}r_1)v^2],$$

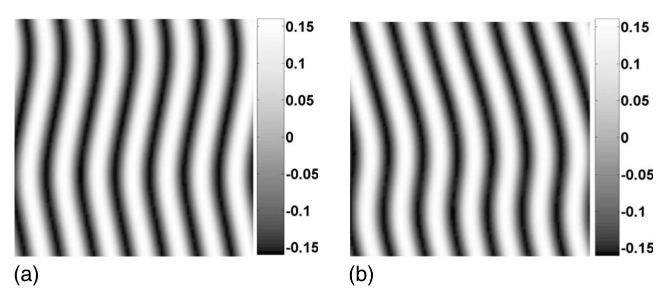

FIG. 5. Turing patterns obtained when (a) α=0.95, β=0.92, r_1=3.5, r_2=0; (b) α=0.92, β=0.88, r_1=3.5, r_2=0.

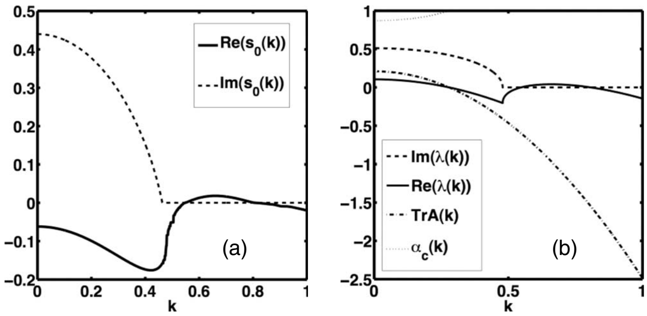

FIG. 6. (a) Zeros of $S(k)$ for $\alpha=0.8<\alpha_c(0)$, using the parameters $a_{11}=0.91$, $a_{22}=-0.7$, $a_{12}=1.0$, $a_{21}=-a_{11}$, $\delta=2$, $D=0.35$. (b) Eigenvalues of $A(k)$ around the stationary state. A plot of the $\mathrm{Tr}A(k)$ and of the function $\alpha_c(k)$ is also shown as a reference.

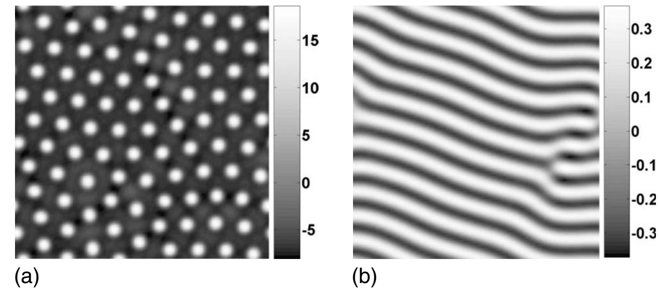

FIG. 7. Turing patterns obtained with $\alpha=\beta=0.8$, $a_{11}=0.91$, $a_{22}=-0.7$, $a_{12}=1$, $a_{21}=-a_{11}$, $\delta=2$, $D=0.35$. (a) $r_2=0.2$, $r_1=0.02$. The pattern converged after 400 000 time steps. (b) $r_2=0$, $r_1=3.5$. The stripes shown correspond to the iteration number 2.7×10^6.

$$\nabla^2 v=-\frac{1}{\delta}[a_{21}u+a_{22}v+r_2uv+(a_{11}r_1)uv^2], \qquad (41)$$

regardless of the presence of subdiffusion.

B. Turing patterns when $\mathrm{Tr}[A(k=0)]>0$

One of the important results reported here is that Turing patterns can develop in a system with $\alpha=\beta<1$ and $\mathrm{Tr}[A(k=0)]>0$. This should open a wider range of possibilities of application of Turing models to biological systems because the restrictive conditions on the parameters imposed by the normal conditions are no longer there, namely, the sign of the cross terms, and of the diagonal terms of the Jacobian are not required to be different [4].

We can demonstrate numerically the formation of Turing patterns when the trace of the Jacobian matrix is positive, and the conditions are those of Eq. (35). Using the values $a_{11}=0.91$, $a_{22}=-0.7$, $a_{12}=1$, $a_{21}=-a_{11}$, $\delta=2$, and $D=035$, the BVAM model satisfies such conditions. The corresponding analysis of the zeros of $S(k)$ is shown in Fig. 6(a). It is important to notice that for these parameters one has that $\mathrm{Re}[\lambda(k)]|_{k=0}>0$, $\mathrm{Im}[\lambda(k)]|_{k=0}\neq 0$, and $h(k_0)<0$. Consequently, for a Turing instability to appear one requires that the anomalous exponent $\alpha<\min[\alpha_c(k)]=\alpha_c(0)=0.8712$. Therefore, we choose $\alpha=0.8$.

In Fig. 6(b), we show the eigenvalue behavior for the former set of parameters. Observe that the real part of the eigenvalues is positive for small k and one should expect that if one performs a numerical calculation of the model with normal diffusion with these parameters, starting with random initial conditions around the uniform state, the solution would oscillate. We have confirmed this statement in numerous calculations.

We have solved numerically the BVAM model using the parameters of Fig. 6 for $\delta=2$ and the nonlinear parameters $r_1=0.02$ and $r_2=0.2$, and $r_1=3.5$, $r_2=0$. The calculation was initialised with a small random perturbation around $(u,v)=(0,0)$. The results are shown in Fig. 7, where the Turing patterns produced are seen to be rather similar to the ones obtained before.

It is important to emphasize that the pattern obtained is also a solution of Eq. (41), and it might be a stable solution of the model with normal diffusion. We have verified that this is indeed the case. This means that there are Turing patterns that are not normally predicted by the usual linear analysis, in particular one never predicts patterns when $\mathrm{Tr}A>0$. Furthermore, the basin of attraction for this stationary pattern is different for the cases of normal and anomalous diffusion. We have investigated this numerically as well, by starting a calculation for normal diffusion using the pattern of Fig. 7 as an initial condition and superimposing a random noise of $\delta u_0=\delta v_0=0.005$. Finally, one can stress that subdiffusion enables one to find a path in phase space to a Turing pattern, starting from a perturbation around the uniform state, which is impossible in the case of normal diffusion.

VI. CONCLUSIONS

We have studied subdiffusion modeled with Caputo fractional time derivatives in reaction-diffusion systems. We investigated the instabilities in such systems for arbitrary values of the anomalous exponents α and β in the range (0, 1) by solving $S(k,s)=0$. The zeros of this function $[s_0(k)]$ provide a good guide to investigate the regions of parameter space in which a Turing instability might be present. Numerical calculations show that Turing patterns are obtained when the real part of $s_0(k)$ is negative for $k=0$, and positive for some value of $k\neq 0$. We also found that in the case $\alpha=\beta<1$, Turing instabilities appear in the same regions of parameter space when Turing patterns are formed with normal diffusion. An important result is that we predict the formation of Turing patterns in new regions of parameter space where the normal Turing conditions are not met. In particular, there is the possibility of forming Turing patterns when $\mathrm{Tr}A(k)>0$, which implies that the condition $\mathrm{sgn}(a_{11})\neq\mathrm{sgn}(a_{22})$ can be relaxed, since the condition $a_{11}+a_{22}<0$ is no longer needed. This result is important, since more general reaction kinetics, not necessarily that of the activator-inhibitor kind, can produce Turing patterns.

In general, the Turing instability analysis can be performed for arbitrary values of the anomalous exponents. The homogeneous state remains stable if the difference between the anomalous exponents is sufficiently small. The critical value of this difference can be calculated numerically, as well as the existence of Turing instabilities when $\mathrm{Tr}A(k)>0$. In this case, to assure the stability of the homogeneous state, the anomalous exponents must fulfill $\alpha,\beta<\alpha_c(0)$, where $\alpha_c(0)$ is the critical value corresponding to the same parameters when $\alpha=\beta$.

The extension of the Turing conditions found here is important, since there should be real biological and chemical systems that do not meet the Turing conditions with normal diffusion, yet meeting these new conditions for anomalous diffusion. As mentioned before, there are many real biological systems that show evidence of anomalous diffusive processes, particularly in living tissues [13,49,50].

It is important to remark that once a Turing pattern is formed it is not possible to know if there is subdiffusion, since the stationary Poisson equation fulfills the same boundary conditions and does not depend on time. We verified that the Turing pattern formed with a system with subdiffusion, and with parameters such that $\mathrm{Tr}A(0)>0$, is stable by performing a numerical calculation in a system with normal diffusion and the same parameters using random deviations around this pattern. The basin of attraction is reasonably large, but it does not contain the uniform state. Perturbations around the uniform state in conditions with normal diffusion do not result in a Turing pattern, but to oscillations of large wavelength. The finding that Turing patterns can be obtained in different ways opens up the possibility of designing new experimental reactors in which the Turing instability could be observed. It is worth emphasizing that most of our results are independent of the particular kinetics used.

Finally, this general study of subdiffusion, together with previous results from other models of subdiffusion and superdiffusion, allows us to conclude that the physical processes that cause anomalous diffusive behaviour favor the formation of Turing patterns.

ACKNOWLEDGMENTS

This work was partially financed by CONACyT project No. 79641. R.A.B wishes to thank the Centre of Mathematical Biology, Mathematical Institute, University of Oxford, where part of this work was carried out. Financial support of a sabbatical grant by DGAPA UNAM and CONACyT, Mexico is fully acknowledged. D.H.H wishes to thank M. Chernicoff for useful discussions about this work.

APPENDIX A: SOLUTION OF THE FRACTIONAL DIFFERENTIAL EQUATION

We need to solve the following equation:

$$\frac{{}^c\partial^\alpha u}{\partial t^\alpha}=\lambda u,$$

$$u(0)=1, \quad 0<\alpha\leqslant 1. \tag{A1}$$

The Caputo fractional derivative [Eq. (9)] is given by

$$\frac{{}^c\partial^\alpha u}{\partial t^\alpha}=\frac{1}{\Gamma(1-\alpha)}\int_0^t (t-\tau)^{-\alpha}\frac{\partial u}{\partial \tau}d\tau. \tag{A2}$$

Taking the Laplace transform and noting that Eq. (A2) is a convolution, we obtain

$$\frac{1}{\Gamma(1-\alpha)}\mathcal{L}(t^{-\alpha})\mathcal{L}\left(\frac{\partial u}{\partial t}\right)=\lambda\mathcal{L}(u) \tag{A3}$$

or

$$\frac{1}{\Gamma(1-\alpha)}[\Gamma(1-\alpha)s^{\alpha-1}][s\hat{u}(s)-1]=\lambda\hat{u}(s). \tag{A4}$$

Solving for $\hat{u}(s)$, we obtain

$$\hat{u}(s)=\frac{s^{\alpha-1}}{s^\alpha-\lambda}. \tag{A5}$$

Taking the inverse transform, we finally arrive at

$$u(t)=\frac{1}{2\pi i}\int_{\sigma-i\infty}^{\sigma+i\infty}\frac{e^{st}s^{\alpha-1}}{s^\alpha-\lambda}ds, \tag{A6}$$

where σ is larger than the real part of all singularities. There are simple poles and a branch cut in the negative real axis. Therefore, we choose the Bromwich contour [51], where the integrals along the circular segments vanish, and the only contributions are along the negative real axis, Γ_2 above and Γ_3 below. Therefore,

$$\begin{aligned}
u(t) &= \sum \mathrm{res}\left(\frac{e^{st}s^{\alpha-1}}{s^\alpha-\lambda}\right)-\frac{1}{2\pi i}\left(\int_{\Gamma_2}\hat{u}(s)e^{st}ds+\int_{\Gamma_3}\hat{u}(s)e^{st}ds\right)\\
&= \sum \mathrm{res}\left(\frac{e^{st}s^{\alpha-1}}{s^\alpha-\lambda}\right)-\frac{1}{2\pi i}\left(\int_{-\infty}^{0}\frac{e^{xte^{i\pi}}x^{\alpha-1}e^{i\pi(\alpha-1)}e^{i\pi}dx}{x^\alpha e^{i\pi\alpha}-\lambda}\right.\\
&\quad\left.+\int_0^\infty\frac{e^{xte^{-i\pi}}x^{\alpha-1}e^{-i\pi(\alpha-1)}e^{-i\pi}dx}{x^\alpha e^{-i\pi\alpha}-\lambda}\right)\\
&= \sum \mathrm{res}\left(\frac{e^{st}s^{\alpha-1}}{s^\alpha-\lambda}\right)-\frac{1}{2\pi i}\left(\int_0^\infty\frac{e^{i\pi\alpha}x^{\alpha-1}e^{-xt}dx}{x^\alpha e^{i\pi\alpha}-\lambda}\right.\\
&\quad\left.-\int_0^\infty\frac{e^{-i\pi\alpha}x^{\alpha-1}e^{-xt}dx}{x^\alpha e^{-i\pi\alpha}-\lambda}\right)\\
&= \sum \mathrm{res}\left(\frac{e^{st}s^{\alpha-1}}{s^\alpha-\lambda}\right)-\frac{\sin(\pi\alpha)}{\pi}\\
&\quad\times\left(\lambda\int_0^\infty\frac{x^{\alpha-1}e^{-xt}dx}{x^{2\alpha}-2\lambda x^\alpha\cos(\pi\alpha)+\lambda^2}\right).
\end{aligned} \tag{A7}$$

The poles are found when $s_0^\alpha-\lambda=0$. That is,

$$s_0^\alpha=|\lambda|^{1/\alpha}e^{i(\theta+2n\pi)/\alpha},$$

$$|(\theta+2n\pi)/\alpha|\leqslant\pi, \quad n\in\mathbb{N}. \tag{A8}$$

However, since $\alpha<1$, then $|(\theta+2n\pi)/\alpha|\leqslant\pi\Rightarrow n=0$. Accordingly, the residue calculation gives

$$\sum \mathrm{res}\left(\frac{e^{st}s^{\alpha-1}}{s^\alpha - \lambda}\right) = \frac{1}{\alpha}\exp(|\lambda|^{1/\alpha}te^{(i\theta/\alpha)}). \quad \text{(A9)}$$

Changing variable $x=|\lambda|^{1/\alpha}r$ and writting $\lambda=|\lambda|e^{i\theta}$ in the last integral of Eq. (A7), we finally arrive at the solution of Eq. (A1),

$$u(t) = \frac{1}{\alpha}\exp(|\lambda|^{1/\alpha}te^{(i\theta/\alpha)}) - \frac{\sin(\pi\alpha)}{\pi}\int_0^\infty \frac{r^{\alpha-1}e^{-|\lambda|^{1/\alpha}rt}dr}{e^{-i\theta}r^{2\alpha} - 2r^\alpha\cos(\pi\alpha) + e^{-i\theta}}. \quad \text{(A10)}$$

[1] A. M. Turing, Philos. Trans. R. Soc. London, Ser. B **237**, 37 (1952).
[2] I. Prigogine and R. Lefever, J. Chem. Phys. **48**, 1695 (1968).
[3] S. A. Gourley and N. F. Britton, J. Math. Biol. **34**, 297 (1996).
[4] J. D. Murray, *Mathematical Biology II*, Vol. 18 of *Interdisciplinary Applied Mathematics* (Springer-Verlag, Berlin, 2003).
[5] R. A. Barrio, *Turing Systems: A General Model for Complex Patterns in Nature*, in *Physics of Emergence and Organization*, edited by I. Licata and A. J. Sakaji (World Scientific, Singapore, 2007).
[6] V. Castets, E. Dulos, J. Boissonade, and P. DeKepper, Phys. Rev. Lett. **64**, 2953 (1990).
[7] S. Kondo and R. Asai, Nature **376**, 765 (1995).
[8] S. Sick, S. Reinker, J. Timmer, and T. Schlake, Science **314**, 1447 (2006).
[9] C. Varea and R. Barrio, J. Phys.: Condens. Matter **16**, S5081 (2004).
[10] G. Drazer and D. H. Zanette, Phys. Rev. E **60**, 5858 (1999).
[11] R. Hilfer, Chem. Phys. **284**, 399 (2002).
[12] I. Goychuk and P. Hänggi, Phys. Rev. E **70**, 051915 (2004).
[13] K. Ritchie, X.-Y. Shan, J. K., K. Iwasawa, T. Fujiwara, and A. Kusumi, Biophys. J. **88**, 2266 (2005).
[14] R. Metzler, J. Klafter, J. Jortner, and M. Volk, Chem. Phys. Lett. **293**, 477 (1998).
[15] G. Zumofen, J. Klafter, and M. Shlesinger, Chem. Phys. **212**, 89 (1996).
[16] M. G. W. Schmidt, F. Sagués, and I. M. Sokolov, J. Phys.: Condens. Matter **19**, 065118 (2007).
[17] B. I. Henry, T. A. M. Langlands, and S. L. Wearne, Phys. Rev. E **72**, 026101 (2005).
[18] B. I. Henry, T. A. M. Langlands, and S. L. Wearne, Phys. Rev. E **74**, 031116 (2006).
[19] V. V. Gafiychuk and B. Y. Datsko, Phys. Rev. E **75**, 055201(R) (2007).
[20] T. A. M. Langlands, B. I. Henry, and S. L. Wearne, J. Phys.: Condens. Matter **19**, 065115 (2007).
[21] R. A. Barrio, C. Varea, J. L. Aragón, and P. K. Maini, Bull. Math. Biol. **61**, 483 (1999).
[22] A. Einstein, Ann. Phys. **322**, 549 (1905).
[23] L. F. Richardson, Proc. R. Soc. London, Ser. A **110**, 709 (1926).
[24] H. Scher and M. Lax, Phys. Rev. B **7**, 4491 (1973).
[25] E. W. Montroll and G. H. Weiss, J. Math. Phys. **6**, 167 (1965).
[26] J. P. Bouchaud and A. Georges, Phys. Rep. **195**, 127 (1991).
[27] J. Klafter, M. F. Shlesinger, and G. Zumofen, Phys. Today **49**, 33 (1996).
[28] A. Compte, Phys. Rev. E **53**, 4191 (1996).
[29] R. Metzler and J. Klafer, Phys. Rep. **339**, 1 (2000).
[30] R. Metzler and J. Klafter, J. Phys. A **37**, R161 (2004).
[31] P. Lévy, *Théorie de l'Addition des Variables Aliétoires* (Guthier-Villars, Paris, 1937).
[32] D. del Castillo-Negrete, B. A. Carreras, and V. E. Lynch, Phys. Rev. Lett. **94**, 065003 (2005).
[33] A. I. Saichev and G. M. Zaslavsky, Chaos **7**, 753 (1997).
[34] D. Ben-Avraham and S. Havlin, *Diffusion and Reactions in Fractals and Disordered Systems* (Cambridge University Press, Cambridge, UK, 2004).
[35] R. Hilfer and L. Anton, Phys. Rev. E **51**, R848 (1995).
[36] M. F. Shlesinger, G. M. Zaslavsky, and J. Klafer, Nature **363**, 31 (1993).
[37] R. Hilfer, Physica A **329**, 35 (2003).
[38] F. Mainardi and R. Gorenflo, J. Comput. Appl. Math. **118**, 283 (2000).
[39] I. Podlubny, *Fractional Differential Equations* (Academic, San Diego, 1999).
[40] V. V. Gafiychuk and B. Datsko, Physica A **365**, 300 (2006).
[41] F. Sagués, V. P. Shkilev, and I. M. Sokolov, Phys. Rev. E **77**, 032102 (2008).
[42] K. Seki, M. Wojcik, and M. Tachiya, J. Chem. Phys. **119**, 7525 (2003).
[43] *Subdiffusion Limited Reaction*, in *Anomalous Transport: Foundations and Aplications*, edited by R. Klages, G. Radons, and I. M. Sokolov (Wiley-VCH, Weinheim, 2007).
[44] G. Hornung, B. Berkowitz, and N. Barkai, Phys. Rev. E **72**, 041916 (2006).
[45] V. Gafiychuk, B. Datsko, and V. Meleshko, e-print arXiv:0611005.
[46] Y. Nec and A. A. Nepomnyaschy, Eur. J. Appl. Math. **19**, 329 (2008).
[47] A. Yadav and W. Horsthemke, Phys. Rev. E **74**, 066118 (2006).
[48] R. Gorenflo and E. A. Abdel-Rehim, J. Comput. Appl. Math. **205**, 871 (2007).
[49] M. Weiss, M. Elsner, F. Kartberg, and T. Nilsson, Biophys. J. **87**, 3518 (2004).
[50] M. Weiss, H. Hashimoto, and T. Nilsson, Biophys. J. **84**, 4043 (2003).
[51] B. I. Henry and S. L. Wearne, SIAM J. Appl. Math. **62**, 870 (2002).